Current Biology 22, 632–637, April 10, 2012 ©2012 Elsevier Ltd All rights reserved DOI 10.1016/j.cub.2012.02.023

Report

Dynein Tethers and Stabilizes Dynamic Microtubule Plus Ends

Adam G. Hendricks,[1,5] Jacob E. Lazarus,[1,5] Eran Perlson,[2] Melissa K. Gardner,[3] David J. Odde,[4] Yale E. Goldman,[1] and Erika L.F. Holzbaur[1,*]

[1]Department of Physiology and the Pennsylvania Muscle Institute, University of Pennsylvania Perelman School of Medicine, Philadelphia, PA 19104-6085, USA

[2]Department of Physiology and Pharmacology, Sackler Faculty of Medicine, Tel Aviv University, Ramat Aviv, Tel Aviv 69978, Israel

[3]Department of Genetics, Cell Biology and Development

[4]Department of Biomedical Engineering

University of Minnesota, Minneapolis, MN 55455, USA

Summary

Microtubules undergo alternating periods of growth and shortening, known as dynamic instability. These dynamics allow microtubule plus ends to explore cellular space. The "search and capture" model posits that selective anchoring of microtubule plus ends at the cell cortex may contribute to cell polarization, spindle orientation, or targeted trafficking to specific cellular domains [1–3]. Whereas cytoplasmic dynein is primarily known as a minus-end-directed microtubule motor for organelle transport, cortically localized dynein has been shown to capture and tether microtubules at the cell periphery in both dividing and interphase cells [3–7]. To explore the mechanism involved, we developed a minimal in vitro system, with dynein-bound beads positioned near microtubule plus ends using an optical trap. Dynein induced a significant reduction in the lateral diffusion of microtubule ends, distinct from the effects of other microtubule-associated proteins such as kinesin-1 and EB1. In assays with dynamic microtubules, dynein delayed barrier-induced catastrophe of microtubules. This effect was ATP dependent, indicating that dynein motor activity was required. Computational modeling suggests that dynein delays catastrophe by exerting tension on individual protofilaments, leading to microtubule stabilization. Thus, dynein-mediated capture and tethering of microtubules at the cortex can lead to enhanced stability of dynamic plus ends.

Results and Discussion

Strong evidence that cortically localized dynein can mediate interactions between microtubules and the cell periphery comes from studies in *S. cerevisiae*, where dynein's primary role is to exert tension on microtubules projecting from the spindle pole body in order to properly position the nucleus at the bud neck [2, 4]. A parallel mechanism also functions in higher eukaryotes, as cortically localized dynein has been implicated in the proper positioning of the spindle in dividing cells in *C. elegans*, *Drosophila*, and human cells [5, 8, 9]. In interphase cells as well, cortically localized dynein mediates microtubule capture and tethering, primarily at sites of cell-cell interaction such as adherens junctions and the immunological synapse [6, 7]. Here, we explored the mechanistic basis of microtubule tethering by mammalian dynein, using in vitro assays employing optical trapping, reconstitution of microtubule dynamics, and total internal reflection fluorescence (TIRF) microscopy.

We first asked whether dynein-bound polystyrene beads could tether projecting microtubule plus ends. We anchored polarity-marked Taxol-stabilized microtubules to a coverslip via their biotinylated seeds, so that the microtubule minus ends were fixed. This geometry allows the unbiotinylated and thus unattached plus ends to undergo lateral diffusive movements (Figure 1A). Then, in the presence of 1 mM MgATP, we used an optical trap to bring dynein- or BSA-coated beads, one at a time, to the mobile plus end of a microtubule. When BSA-coated beads were brought near the microtubule plus end, the variance in the lateral position did not decrease (Figure 1B; see also Movie S1 available online). In contrast, when dynein-coated beads were brought near the microtubule plus end, the microtubule became tethered, resulting in a pronounced decrease in the variance in the lateral position of the microtubule tip (Figure 1B; Movie S1).

When released from the trap, beads moved toward the minus end, consistent with dynein motor function (Figure S1). We used the optical trap to measure the force exerted by the dynein-bound beads on microtubules stably attached to the coverslip along their length and found forces ranging from 2 to 8 pN (Figure 1C). Because mammalian cytoplasmic dynein has a unitary stall force of ~1.1 pN and the force applied by multiple dynein motors is close to additive under these conditions [10, 11], this suggests that two to eight dynein motors may simultaneously interact with an individual microtubule in this assay.

Next, we asked whether these effects were unique to dynein or whether other microtubule-associated proteins might have the same effect of dampening the lateral mobility of the microtubule plus end, consistent with tethering. We independently compared the effects of either purified recombinant kinesin-1 or the plus-end-tracking protein EB1 on microtubule mobility using the optical trap assay. Both kinesin-1- and EB1-bound beads were able to bind to the microtubule, decreasing the lateral variance of the microtubule plus end as compared to BSA-bound control beads. However, neither kinesin-1 nor EB1 decreased the lateral variance of the microtubule as effectively as dynein (Figure 1D). Furthermore, we observed distinct effects of these proteins on the microtubule plus end relative to dynein (Movie S1). While the microtubule remained in contact with the bead, the plus end continued to "search" the surface of either kinesin-1-bound or EB1-bound beads, resulting in less-effective tethering (Movie S1). In the case of kinesin-1, we occasionally observed microtubule buckling, consistent with the application of a compressive load on the microtubule by a plus-end-directed motor. This was not seen with EB1-bound beads, where the microtubule plus end remained in contact with the bead but continued to search the surface (Movie S1), likely due to individual binding and release events from multiple EB1 molecules bound to the bead

[5]These authors contributed equally to this work

*Correspondence: holzbaur@mail.med.upenn.edu

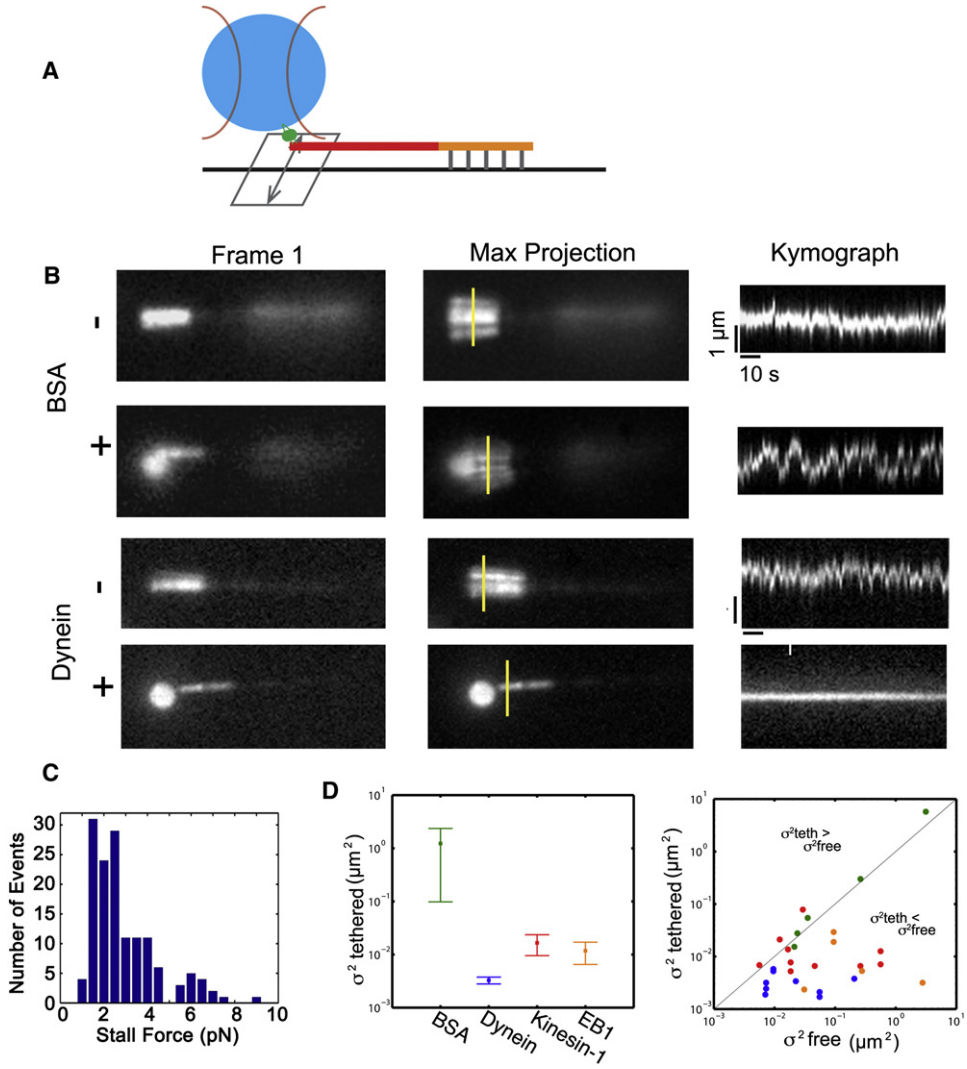

Figure 1. Dynein Tethers Microtubule Plus Ends In Vitro

(A) Microtubules polymerized from dimly labeled, biotinylated seeds were attached to a coverslip via an anti-biotin antibody. The bright, plus ends of the microtubule were not biotinylated and thus free to diffuse.

(B) BSA-coated beads do not decrease the lateral variance of the microtubule plus end. Shown are the initial frame of the movie, the maximum projection image of the sequence, and kymographs taken along the yellow line segments, showing variation in lateral position over time. In contrast, interactions with dynein-bound beads result in decreased lateral mobility of microtubule plus ends.

(C) Histogram of stall forces for dynein-bound beads interacting with stably bound microtubules. Stall forces ranged from 2 to 8 pN, suggesting that two to eight dynein motors on the bead are able to simultaneously interact with a microtubule.

(D) Dynein-bound beads induce stable microtubule tethering, as indicated by the variance in the presence ($\sigma^2_{tethered}$) of the bead. For kinesin-1 and EB1, the microtubule searches the bead surface, resulting in greater lateral diffusion. Error bars indicate SEM. The scatter plot compares the lateral diffusion in the presence ($\sigma^2_{tethered}$) or absence (σ^2_{free}) of the bead.

See also Figure S1 and Movie S1.

surface. In contrast, dynein-bound beads induced a more stable attachment with the microtubule end, exerting tension that appeared to stiffen the microtubule, decreasing lateral fluctuations along its length (Movie S1).

Microtubules in the cell are dynamic, undergoing periods of growth and shrinkage known as dynamic instability due to the addition and loss of tubulin subunits, primarily at their plus ends [12]. These dynamics allow the plus ends to sample the cytoplasm over time, exploring cellular space. We next asked whether dynein-bound beads could tether dynamic microtubule plus ends (Figure 2A). In a flow chamber maintained at 37°C, we bound biotinylated microtubule seeds and BSA- or dynein-coated beads to the coverglass surface. We next added 10 μM tubulin dimers to the chamber, reconstituting dynamic instability. Microtubule dynamics were monitored by TIRF microscopy.

Interactions of dynamic microtubules with BSA-coated beads often led to rapid catastrophe in this assay (Figure 2B; Movie S2), consistent with previous observations demonstrating induction of catastrophe by contact with a rigid barrier [13]. In contrast, microtubules that encountered dynein-bound beads in the presence of ATP did not often undergo catastrophe. Instead, the initial encounter of the microtubule with the bead was stabilized. In some encounters with

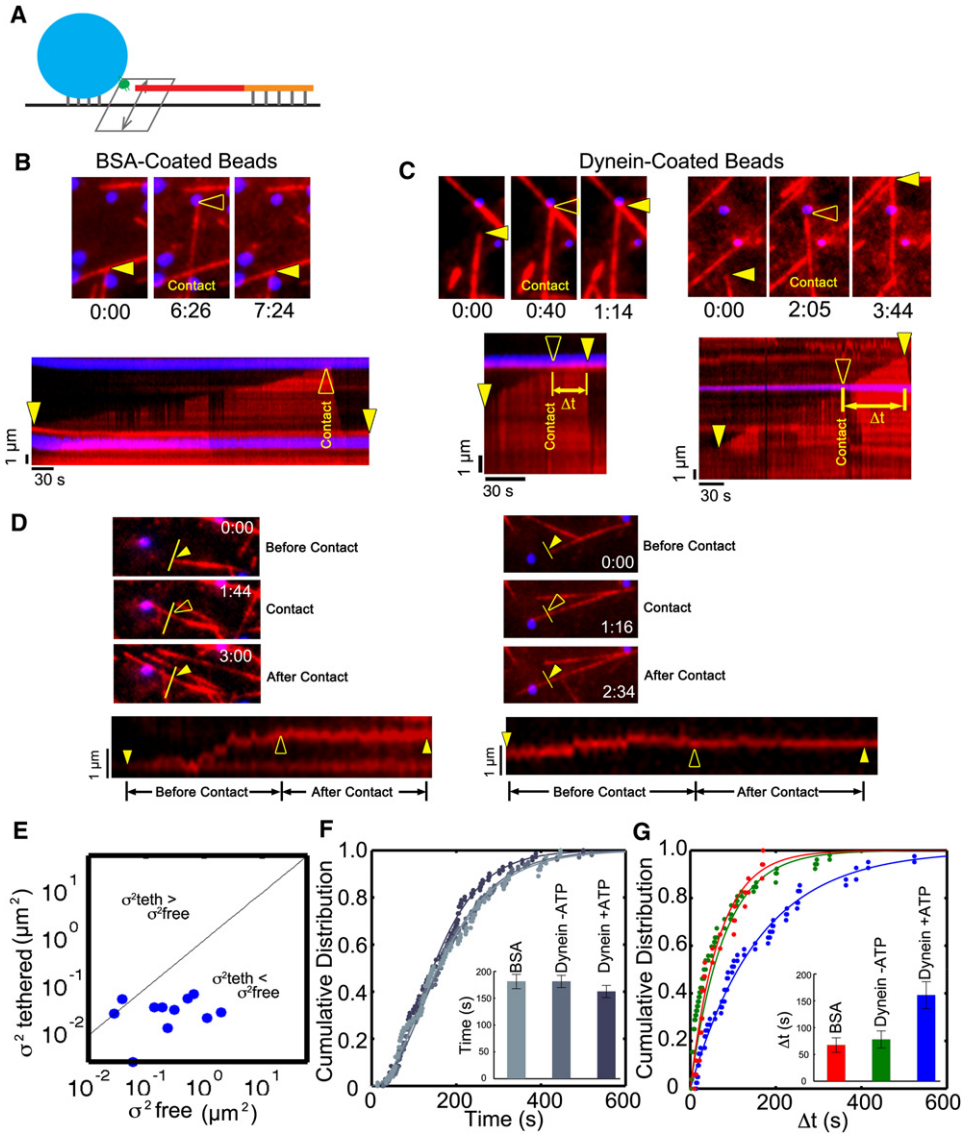

Figure 2. Dynein-Mediated Tethering of Dynamic Microtubule Plus Ends Is ATP Dependent

(A) Dynein- or BSA-bound beads and biotinylated microtubule seeds were attached to the surface of a flow chamber, and microtubule polymerization was initiated by the introduction of 10 μM tubulin. Interactions of growing microtubule plus ends with protein-bound beads were monitored over time.

(B) Dynamic microtubules contacting BSA-coated beads rapidly undergo catastrophe. A time series is shown at the top, with the point of contact highlighted by the open arrowhead. A corresponding kymograph is shown below; the solid arrowheads mark initial and final positions of the microtubule end, and the open arrowhead marks the point of contact with the bead.

(C) In contrast, microtubules become tethered when encountering dynein-coated beads, as measured by an increased time to catastrophe (Δt). Closed arrowheads mark initial and final positions of the microtubule plus end, and open arrowheads mark the point of contact with the bead.

(D) Two examples of the effects of dynein-mediated tethering on the lateral variance of dynamic microtubules. Time series (top three panels) and corresponding kymographs (bottom panels, taken along the indicated yellow line) show that interaction with dynein-coated beads reduces the lateral diffusion of the growing microtubule. Solid arrowheads mark the starting and ending positions, and the open arrowhead marks the initiation of contact with the bead. In the kymograph on the left, note that the bottom line results from the intersection of a second microtubule with the yellow line.

(E) Lateral diffusion for growing microtubules before (σ^2_{free}) and after ($\sigma^2_{tethered}$) contact with dynein-bound beads.

(F) Time to catastrophe for microtubules that do not contact beads is similar across different experimental conditions. Solid lines show fits to a gamma distribution. Error bars indicate SEM.

(G) The mean time between initial contact with the bead and catastrophe for dynein-coated beads in the presence of 1 mM MgATP is significantly longer than for encounters with a dynein-coated bead in the absence of ATP or with a BSA-coated bead ($p < 0.02$). Solid lines show fits to a single exponential. Error bars indicate SEM.

See also Figure S2 and Movies S2 and S3.

dynein-bound beads, the microtubule remained tethered (Figure 2C, left panels). In other encounters, the microtubule plus end continued to polymerize past the bead while bead-bound dynein maintained a lateral interaction with the microtubule lattice (Figure 2C, right panels; see also Movie S3). Importantly, when a growing microtubule plus end encountered a dynein-bound bead in the presence of 1 mM ATP, we observed a marked decrease in the variance of lateral position

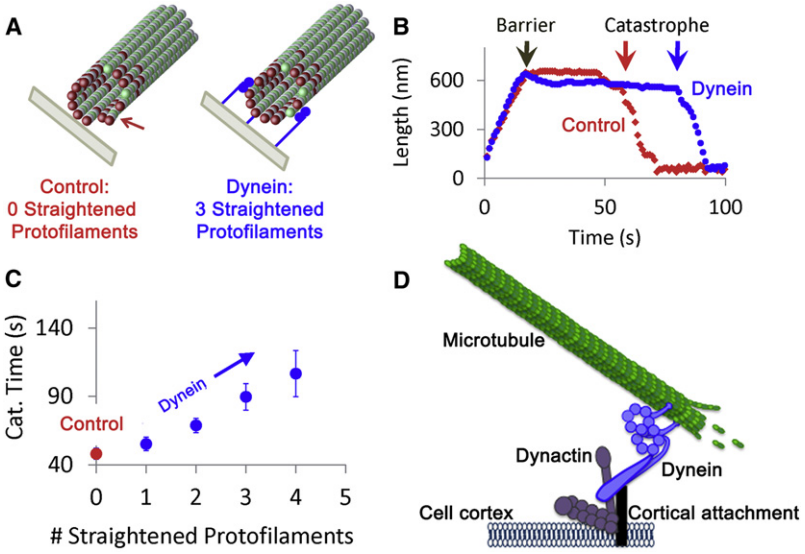

Figure 3. Cortically Localized Dynein Tethers and Stabilizes Microtubules

(A) Three-dimensional model simulations assume that GDP-tubulin subunits (green, with GTP-tubulin subunits in red) have an intrinsic preference for curving outward in the microtubule lattice, and so extended protofilaments with exposed GDP-tubulin subunits near the tip have the tendency to curl outwardly (left). This curling destabilizes the microtubule tip, leading to catastrophe events. However, cortex-anchored dynein could straighten individual protofilaments as dynein exerts tension on the microtubule tip (right, three dynein molecules shown in blue).

(B) In the 3D model simulations, once a microtubule contacts the barrier, the microtubule has a catastrophe event after ~30 s in this simulation run. However, if three random protofilaments are targeted for straightening in the simulation, the time to undergo a catastrophe event is increased to ~70 s.

(C) The mean simulated time to catastrophe after contact with a barrier is given as a function of the number of protofilaments that are targeted for straightening in the simulation. For three targeted protofilaments, simulated catastrophe time increases about 2-fold, consistent with experimental observations. Error bars indicate SEM.

(D) In a proposed model, cortically anchored dynein can actively tether and stabilize projecting microtubule plus ends.

consistent with dynein-mediated tethering (Figures 2D and 2E), similar to the dynein-mediated tethering observed in the optical trap assays (Figure 1B).

To determine the effects of dynein-mediated tethering on microtubule stability, we measured the time from initial contact to catastrophe for dynein-coated beads as compared to control beads. We found that in the presence of ATP, the mean time from contact to catastrophe was 161 ± 25 s for dynein-bound beads, as compared to 67 ± 13 s for BSA-coated beads (Figures 2G and S2; $p < 0.02$). Only microtubules making direct contact with beads were affected: no significant differences were detected in microtubule dynamics away from the beads under any of the conditions tested (Figure 2F).

Strikingly, although dynein is known to bind tightly to microtubules in the absence of ATP (apo state), encounters between microtubule ends and dynein-coated beads in the absence of ATP were not significantly different from those of microtubule ends encountering BSA-coated beads (Figure 2G; $p > 0.7$). Thus, the ATP-dependent motor activity of dynein, and not just the high-affinity binding of dynein to microtubules, is required to stabilize interactions of dynamic microtubules with a barrier.

To further probe the tethering mechanism of dynein, we adapted a previously described three-dimensional computational model that explicitly considers the forces within the microtubule lattice exerted through lateral and longitudinal bonds between each tubulin subunit [14, 15] (Figure 3A). In this model, the nucleotide state of each tubulin subunit determines its preferred angle in the microtubule lattice: GTP-bound tubulin subunits form straight protofilaments, whereas protofilaments with GDP-tubulin subunits tend to curl outwardly when exposed [16], destabilizing the polymer and encouraging catastrophe (Figure 3A). We hypothesized that minus-end-directed dynein can stabilize microtubule plus ends by exerting tension to straighten curled microtubule protofilaments. The force required to straighten a single protofilament is ~1.25 pN [17, 18], similar to the unitary stall force of mammalian dynein (~1.1 pN; [11, 19, 20]). We simulated this situation by allowing microtubule tips to grow against a barrier (Figure 3A) and then randomly selected individual protofilaments to be straightened by the action of dynein pulling near the plus end. We found that the time to undergo a catastrophe event was prolonged when dynein applied force to straighten individual protofilaments (Figure 3B). The length of time that a microtubule plus end was stabilized (time to catastrophe) was found to increase as a function of the number of protofilaments that were acted on by dynein (Figure 3C).

These simulations predict that minus-end-directed dynein motors that are anchored at the cell cortex can transiently stabilize microtubule plus ends and delay catastrophe events by straightening individual protofilaments, resulting in dampened microtubule dynamics. Interestingly, the model predicts that the number of engaged dynein motors required to stabilize microtubules is similar to the number of engaged motors estimated in our in vitro optical trap assays. Thus, even substoichiometric levels of dynein (one to four molecules interacting with a 13-protofilament microtubule) would be expected to appreciably suppress catastrophe by counteracting the initial deforming force exerted on the microtubule as it encounters an organelle or the plasma membrane. Both the data and simulations predict that this stabilization requires active force production—high-affinity binding alone would not be sufficient for this sort of microtubule capture, i.e., where catastrophe is delayed.

Our observations are consistent with previous observations that encounters between a growing microtubule plus end and a rigid barrier induce catastrophe [13]. However, we show that when dynein is present, the microtubule plus end is stabilized, allowing the microtubule to continue to polymerize past the bead barrier. This stabilization requires dynein motor activity, because the observed stabilization is ATP dependent. Thus, active generation of tension is required. Computational modeling suggests that dynein stabilizes the dynamic microtubule plus end through exertion of tension to straighten individual protofilaments. Also, active dynein motors may continuously remodel the connection between the microtubule and

barrier, allowing the productive formation of a lateral contact as the microtubule grows past the bead.

The mechanochemistry of cytoplasmic dynein may be uniquely suited for a role in microtubule tethering. Mammalian cytoplasmic dynein has a relatively low stall force [11, 19, 20] compared to other motors such as kinesin-1, and a variable stepping pattern along the microtubule that includes both sideways and backward steps [21, 22]. The nature of the tethering may also be affected by the number of dynein motors acting on a microtubule plus end. Both our trapping assays and our simulations predict that substoichiometric levels of dynein (one to four molecules interacting with a 13-protofilament microtubule) would suppress catastrophe by counteracting the initial deforming force exerted on the microtubule as it encounters the plasma membrane. However, either the activation of cortical dynein [23] or the recruitment of additional dynein motors to the cortex may lead to modulation of microtubule plus-end dynamics at the cell cortex.

Importantly, these results indicate that dynein not only captures and tethers dynamic microtubule plus ends but can also stabilize these ends and thus modulate microtubule dynamics. This influence on microtubule dynamics may promote the stabilization of specific microtubules, which could serve as preferred tracks for intracellular transport between cell center and subdomains at the cell periphery. As both motor and tether, dynein can also exert force on the cytoskeleton relative to the cortex. This mechanism is critical to spindle positioning in a number of systems [2, 24], as dynein can mediate the association of astral microtubules with the cell cortex in dividing cells. However, dynein has also been localized to the cell cortex at sites of cell-cell adhesion [6, 7]. Microtubule tethering at these sites may facilitate a connection between the dynamic microtubule cytoskeleton and intercellular adhesion molecules, creating a powerful mechanism for cells to react to stimuli in the extracellular environment (Figure 3D). However, further studies to assess the role of dynein in mediating intercellular interactions will be necessary to determine whether the critical function of dynein at these sites is facilitated trafficking or the transduction of force.

Experimental Procedures

Protein Purification

Cytoplasmic dynein and tubulin were purified from bovine brain as described previously [25, 26]. Labeled tubulin was purchased from Cytoskeleton, Inc. Recombinant kinesin-1 (K560) and EB1 were expressed in *E. coli* and purified as described previously [12, 27].

In Vitro Tethering Assays

Polarity-marked microtubules were prepared by polymerizing brightly labeled tubulin onto more dimly labeled, biotinylated, Taxol-stabilized microtubule seeds. Flow chambers were constructed with a silanized coverslip and a glass slide. Biotinylated microtubules were bound to the coverslip with anti-biotin (Sigma, clone BN-34). Chambers were blocked with pluronic F-127 (Sigma) and then rinsed with 2–3 chamber volumes of motility assay buffer (MAB: 10 mM PIPES, 50 mM K+ acetate, 4 mM $MgCl_2$, 1 mM EGTA [pH 7.0], supplemented with 20 μM Taxol). Protein A-coated beads (polystyrene, 1 μm diameter, Polysciences) were incubated with either BSA or dynein [28] on ice for 10 min. Beads were diluted in motility buffer (MAB supplemented with 0.6 mg/ml BSA, 6 mM DTT, 10 mg/ml glucose, 1 μg/ml glucose oxidase, 0.5 μg/ml catalase, 1 mM ATP, 20 μM Taxol) and added to the chamber. The sample was illuminated using a 532 nm laser and imaged with an EM-CCD camera (Photometrics Cascade II). The lateral thermal fluctuations of the nonbiotinylated plus ends of microtubules were observed. Then, an optical trap was used to position a dynein- or BSA-coated bead to interact with the plus end of the microtubule. Kymographs of lateral diffusion were prepared in ImageJ at the same axial location along the microtubule before and after introduction of the bead. A custom MATLAB routine was used to calculate the variance of positions from each kymograph. Independent force traces were acquired using an optical trap [29] for dynein-bound beads interacting with microtubules stably bound to the coverslip. The following criteria were used to identify stalls in the force trace data: stall force > 0.5 pN, stall plateau time > 10 ms, pre-stall velocity > 50 nm/s, snapback velocity > 100 nm/s.

TIRF Assays for Microtubule Dynamics

Microscopy chambers were prepared and dynein was purified as above. YG Beads (polystyrene, 1 μm diameter, Polysciences) were incubated with biotinylated BSA and protein A and attached to the coverslip via anti-biotin. Dynein or BSA was then bound to the beads, followed by washing with 3 chamber volumes. Biotinylated microtubule seeds stabilized with GMPCPP (Jena Biosciences) were incubated in the chamber in polymerization buffer (80 mM K-PIPES, 1 mM $MgCl_2$, 1 mM EGTA, 1 mM ATP, 3 mg/ml BSA [pH 6.8]); the chamber was then washed to remove unbound seeds. Polymerization was initiated with 10 μM tubulin in polymerization buffer supplemented with 0.15% methyl cellulose, 0.5% F-127, 5% deoxy enzyme mix, 22.5 mg/ml glucose, 50 mM DTT, 3 mM GTP. For the no-ATP condition, ATP was not included in the buffers and residual ATP was depleted with a hexokinase-glucose system. Objective-type TIRF illumination (Nikon Ti with house-built TIRF illuminator and 1.49 NA apochromatic TIRF objective) was used to image the microtubules and beads. Images were collected every 2 s using an EM-CCD camera (Photometrics Cascade II) and analyzed in ImageJ.

Computational Modeling

Three-dimensional computational simulations of microtubule assembly were developed using MATLAB as described previously [30]. Briefly, outward curling of GDP-tubulin subunits when exposed at a microtubule tip leads to mechanical strain between neighboring tubulin subunits, thus reducing the stability of the subunits in the lattice. Simulations were performed by allowing microtubules to grow for ~20 s real time before contacting a stiff barrier that stalled further growth [15]. The time to a catastrophe event was then recorded for each microtubule. To simulate protofilament straightening mediated by dynein, we adjusted the GDP-tubulin preferred angle to 0 degrees (rather than 22 degrees) for an assigned number of randomly selected protofilaments. Three to twenty-five events were simulated for each case.

Supplemental Information

Supplemental Information includes two figures and three movies and can be found with this article online at doi:10.1016/j.cub.2012.02.023.

Acknowledgments

We thank Benjamin Stevens and Pritish Argawal for scientific and technical assistance. This work was supported by NIH grant GM48661 to E.L.F.H., NIH grant GM71522 and NSF grant 0615568 to D.J.O., a Muscular Dystrophy Association postdoctoral fellowship to E.P., an NIH postdoctoral fellowship to A.G.H., and an NIH predoctoral fellowship to J.E.L. The optical trap was funded by NSF Nanotechnology Science and Engineering Center grant DMR04-25780 and NIH grant GM087253.

Received: September 6, 2011
Revised: February 1, 2012
Accepted: February 10, 2012
Published online: March 22, 2012

References

1. Kirschner, M., and Mitchison, T. (1986). Beyond self-assembly: from microtubules to morphogenesis. Cell *45*, 329–342.
2. Moore, J.K., and Cooper, J.A. (2010). Coordinating mitosis with cell polarity: Molecular motors at the cell cortex. Semin. Cell Dev. Biol. *21*, 283–289.
3. Levy, J.R., and Holzbaur, E.L. (2007). Special delivery: dynamic targeting via cortical capture of microtubules. Dev. Cell *12*, 320–322.
4. Heil-Chapdelaine, R.A., Oberle, J.R., and Cooper, J.A. (2000). The cortical protein Num1p is essential for dynein-dependent interactions of microtubules with the cortex. J. Cell Biol. *151*, 1337–1344.

5. Gönczy, P., Pichler, S., Kirkham, M., and Hyman, A.A. (1999). Cytoplasmic dynein is required for distinct aspects of MTOC positioning, including centrosome separation, in the one cell stage Caenorhabditis elegans embryo. J. Cell Biol. *147*, 135–150.
6. Ligon, L.A., Karki, S., Tokito, M., and Holzbaur, E.L. (2001). Dynein binds to beta-catenin and may tether microtubules at adherens junctions. Nat. Cell Biol. *3*, 913–917.
7. Combs, J., Kim, S.J., Tan, S., Ligon, L.A., Holzbaur, E.L., Kuhn, J., and Poenie, M. (2006). Recruitment of dynein to the Jurkat immunological synapse. Proc. Natl. Acad. Sci. USA *103*, 14883–14888.
8. Siller, K.H., and Doe, C.Q. (2009). Spindle orientation during asymmetric cell division. Nat. Cell Biol. *11*, 365–374.
9. Samora, C.P., Mogessie, B., Conway, L., Ross, J.L., Straube, A., and McAinsh, A.D. (2011). MAP4 and CLASP1 operate as a safety mechanism to maintain a stable spindle position in mitosis. Nat. Cell Biol. *13*, 1040–1050.
10. Mallik, R., Carter, B.C., Lex, S.A., King, S.J., and Gross, S.P. (2004). Cytoplasmic dynein functions as a gear in response to load. Nature *427*, 649–652.
11. Schroeder, H.W., 3rd, Mitchell, C., Shuman, H., Holzbaur, E.L., and Goldman, Y.E. (2010). Motor number controls cargo switching at actin-microtubule intersections in vitro. Curr. Biol. *20*, 687–696.
12. Dixit, R., Barnett, B., Lazarus, J.E., Tokito, M., Goldman, Y.E., and Holzbaur, E.L. (2009). Microtubule plus-end tracking by CLIP-170 requires EB1. Proc. Natl. Acad. Sci. USA *106*, 492–497.
13. Janson, M.E., de Dood, M.E., and Dogterom, M. (2003). Dynamic instability of microtubules is regulated by force. J. Cell Biol. *161*, 1029–1034.
14. VanBuren, V., Cassimeris, L., and Odde, D.J. (2005). Mechanochemical model of microtubule structure and self-assembly kinetics. Biophys. J. *89*, 2911–2926.
15. Schek, H.T., 3rd, Gardner, M.K., Cheng, J., Odde, D.J., and Hunt, A.J. (2007). Microtubule assembly dynamics at the nanoscale. Curr. Biol. *17*, 1445–1455.
16. Wang, H.W., and Nogales, E. (2005). Nucleotide-dependent bending flexibility of tubulin regulates microtubule assembly. Nature *435*, 911–915.
17. Grishchuk, E.L., Efremov, A.K., Volkov, V.A., Spiridonov, I.S., Gudimchuk, N., Westermann, S., Drubin, D., Barnes, G., McIntosh, J.R., and Ataullakhanov, F.I. (2008). The Dam1 ring binds microtubules strongly enough to be a processive as well as energy-efficient coupler for chromosome motion. Proc. Natl. Acad. Sci. USA *105*, 15423–15428.
18. Gardner, M.K., Pearson, C.G., Sprague, B.L., Zarzar, T.R., Bloom, K., Salmon, E.D., and Odde, D.J. (2005). Tension-dependent regulation of microtubule dynamics at kinetochores can explain metaphase congression in yeast. Mol. Biol. Cell *16*, 3764–3775.
19. Mallik, R., Petrov, D., Lex, S.A., King, S.J., and Gross, S.P. (2005). Building complexity: an in vitro study of cytoplasmic dynein with in vivo implications. Curr. Biol. *15*, 2075–2085.
20. Soppina, V., Rai, A.K., Ramaiya, A.J., Barak, P., and Mallik, R. (2009). Tug-of-war between dissimilar teams of microtubule motors regulates transport and fission of endosomes. Proc. Natl. Acad. Sci. USA *106*, 19381–19386.
21. Ross, J.L., Shuman, H., Holzbaur, E.L., and Goldman, Y.E. (2008). Kinesin and dynein-dynactin at intersecting microtubules: motor density affects dynein function. Biophys. J. *94*, 3115–3125.
22. Ross, J.L., Wallace, K., Shuman, H., Goldman, Y.E., and Holzbaur, E.L. (2006). Processive bidirectional motion of dynein-dynactin complexes in vitro. Nat. Cell Biol. *8*, 562–570.
23. Markus, S.M., and Lee, W.L. (2011). Regulated offloading of cytoplasmic dynein from microtubule plus ends to the cortex. Dev. Cell *20*, 639–651.
24. Laan, L., Pavin, N., Husson, J., Romet-Lemonne, G., van Duijn, M., López, M.P., Vale, R.D., Jülicher, F., Reck-Peterson, S.L., and Dogterom, M. (2012). Cortical dynein controls microtubule dynamics to generate pulling forces that position microtubule asters. Cell *148*, 502–514.
25. Bingham, J.B., King, S.J., and Schroer, T.A. (1998). Purification of dynactin and dynein from brain tissue. Methods Enzymol. *298*, 171–184.
26. Castoldi, M., and Popov, A.V. (2003). Purification of brain tubulin through two cycles of polymerization-depolymerization in a high-molarity buffer. Protein Expr. Purif. *32*, 83–88.
27. Dixit, R., Ross, J.L., Goldman, Y.E., and Holzbaur, E.L. (2008). Differential regulation of dynein and kinesin motor proteins by tau. Science *319*, 1086–1089.
28. Perlson, E., Jeong, G.B., Ross, J.L., Dixit, R., Wallace, K.E., Kalb, R.G., and Holzbaur, E.L. (2009). A switch in retrograde signaling from survival to stress in rapid-onset neurodegeneration. J. Neurosci. *29*, 9903–9917.
29. Takagi, Y., Homsher, E.E., Goldman, Y.E., and Shuman, H. (2006). Force generation in single conventional actomyosin complexes under high dynamic load. Biophys. J. *90*, 1295–1307.
30. VanBuren, V., Odde, D.J., and Cassimeris, L. (2002). Estimates of lateral and longitudinal bond energies within the microtubule lattice. Proc. Natl. Acad. Sci. USA *99*, 6035–6040.